Title

Biomarkers of disease can be detected in mice as early as 4 weeks after initiation of exposure to third-hand smoke levels equivalent to those found in homes of smokers.

Journal

Clinical Science, 131(19)

ISSN

0143-5221

Authors

Adhami, Neema
Chen, Yuxin
Martins-Green, Manuela

Publication Date

2017-10-01

DOI

10.1042/cs20171053

Peer reviewed

Clinical Science (2017) **131** 2409–2426
DOI: 10.1042/CS20171053

PORTLAND PRESS

Research Article

Biomarkers of disease can be detected in mice as early as 4 weeks after initiation of exposure to third-hand smoke levels equivalent to those found in homes of smokers

Neema Adhami*, Yuxin Chen* and Manuela Martins-Green

Department of Cell Biology and Neuroscience, University of California, Riverside, CA 92521, U.S.A.

Correspondence: Manuela Martins-Green (manuela.martins@ucr.edu)

Third-hand smoke (THS) is a newly discovered environmental health hazard that results from accumulation and aging of second-hand smoke (SHS) toxins on surfaces where smoking has occurred. Our objective was to determine whether there is a time-dependent effect of THS exposure on health. Using an *in vivo* exposure mouse system that mimics exposure of humans to THS, we investigated its effects on biomarkers found in serum, and in liver and brain tissues. Mice were exposed to THS for 1, 2, 4, or 6 months and brain, liver, and serum were collected. We found that THS exposure, as early as 1 month, resulted in increased circulating inflammatory cytokines, tumor necrosis factor by an order of magnitude of 2 and granulocyte macrophage colony-stimulating factor by an order of magnitude of 1.5 and in increases in the stress hormone epinephrine and the liver damage biomarker aspartate aminotransferase (AST), increased in magnitude 1.5 and 2.5 times compared with controls, respectively. THS exposure for 2 months resulted in further damage and at 4 and 6 months, many factors related to oxidative stress were altered and caused molecular damage. We also found that the mice became hyperglycemic and hyperinsulinimic suggesting that insulin resistance (IR) may be a significant consequence of long-term exposure to THS. In *conclusion*, time-dependent THS exposure has a significant effect on health as early as 1 month after initiation of exposure and these alterations progressively worsen with time. Our studies are important because virtually nothing is known about the effects of increased THS exposure time, they can serve to educate the public on the dangers of THS, and the biomarkers we identified can be used in the clinic, once verified in exposed humans.

Introduction

Cigarette toxins affect biological processes as well as organ systems and are detrimental to human health [1,2]. However, most of the emphasis on the dangers of cigarette-smoke exposure has been centered on first-hand smoke (FHS) and second-hand smoke (SHS). FHS is the smoke inhaled directly by the smoker whereas SHS consists of the smoke and toxins emitted when the smoker exhales the smoke of the cigarette into the air, as well as the smoke that is released from the burning end of a cigarette. SHS exposure occurs when people are in the vicinity of someone smoking. A new form of exposure to cigarette toxins is known as the third-hand smoke (THS). THS consists of deposition of SHS toxins on surfaces such as, household upholstery, bedding, carpeting, and furniture where smoking has occurred as well as the clothing, skin, and hair of people who have smoked. These toxins accumulate and age by reacting with the ambient air and changing into carcinogenic chemicals such as tobacco-specific nitrosamines [3]. These toxins cannot be seen but can be smelled and remain on surfaces for many years, resistant to even strong cleaning agents

*These authors contributed equally to this work.

Received: 28 May 2017
Revised: 08 August 2017
Accepted: 09 August 2017

Version of Record published: 15 September 2017

Clinical Science (2017) **131** 2409–2426
DOI: 10.1042/CS20171053

[4]. Therefore, THS people are usually unaware that they are being exposed. Bystanders inhale not only the contaminated air but also are exposed to THS by absorption through the skin [4]. Children are at the highest risk because they are in close contact with household surfaces, they frequently put their hands in their mouths, and have a high surface-to-volume ratio leading to the absorption of these toxins through the skin very effectively. In fact, children living in homes where smoking has occurred contain tobacco metabolites in their urine [5].

We have developed a model system in which the exposure of animals to THS mimics that of human exposure [6]. We found that THS causes alterations in multiple organ systems such as liver, lung, skeletal muscle, and healing of wounds which show various biomarkers of disease [6-9]. In the liver, we found that THS leads to increased lipid levels, indicating non-alcoholic fatty liver disease (NAFLD). This results in increased lipid levels in circulation that potentially contribute to cardiovascular disease. Furthermore, dyslipidemia can result in increased inflammation that could result in development of cirrhosis [10-12]. In the lung, collagen production is increased in addition to the increase in the levels of inflammatory cytokines, suggesting the potential development of fibrosis with implications for inflammation-induced diseases such as chronic obstructive pulmonary disease and asthma [13-14]. In the skin, healing of wounds mimics poor healing of surgical incisions observed in human smokers with an increased propensity of the wound to re-open [15]. In the brain, we find alterations in behavior, including increased hyperactivity [6]. In addition, mice develop hyperinsulinemia, yet they cannot effectively clear glucose from the blood, leading to hyperglycemia as a result of molecular changes in the insulin–insulin receptor signaling pathway [7]. When exposed to THS and fed a high-fat and carbohydrate diet ('western type diet'), these molecular changes and symptoms of insulin resistance (IR) become worse. THS exposure also increases the levels of proinflammatory cytokines in the serum, including the interleukins 1, 4, 6, tumor necrosis factor α (TNF-α), and granulocyte macrophage colony-stimulating factor (GM-CSF), which suggests that the body is in a proinflammatory state. Finally, the most striking attribute that we observe in mice exposed to THS is a generalized increase in oxidative stress and a decrease in the antioxidant enzymes, catalase, and glutathione peroxidase (GPx) in most of the tissues [7]. As a result, we observe oxidative stress mediated damage to DNA, proteins, and lipids [7,9].

It is now important to determine what is the minimum time of exposure to THS required to identify key diagnostic biomarkers of damage and disease associated with THS exposure. These biomarkers, once validated in humans, can be used as critical indicators of exposure to THS, and how long this exposure has occurred. Ideally, in a clinical setting, urine or blood samples can be taken from children that are suspected to be sick because of THS exposure to determine, when, how long, and how much damage THS has caused. For these studies, we exposed different cohorts of mice to THS for 1, 2, 4, and 6 months and then tested these mice for hormonal alterations, IR, metabolic syndrome, and oxidative stress mediated damage to the liver (because it is the detoxifying organ) and to the brain because of the previously observed behavioral changes. Our findings are significant because they show critical times needed for THS exposure to cause health problems and have the potential to be used as diagnostic tools to detect THS exposure in humans, especially children.

Materials and methods

Animals

Male C57BL/6 mice were exposed to THS for 1, 2, 4, 6, months starting at weaning. Age-matched control mice were kept in clean air. Both control and THS-exposed mice were maintained under controlled environmental conditions – 12-h light/dark cycle in conventional cages with *ad libitum* access to standard chow (percent calories: 58% carbohydrate, 28.5% protein, and 13.5% fat) and water.

Ethics statement

All animal experimental protocols were approved by the University of California, Riverside, Institutional Animal Care and Use Committee (UCR-IACUC). Mice were killed by carbon dioxide (CO_2) inhalation, which is the most common method of killing used by NIH. The amount and length of CO_2 exposure were approved by UCR-IACUC.

THS exposure method

Common household fabrics such as curtain material, upholstery, and carpet were placed in empty mouse cages and exposed to SHS generated by the Teague smoking machine as previously described [16]. Each cage contained 10 g of curtain material (cotton), 10 g of upholstery (cotton and fiber), and two 16 in^2 pieces of carpet (fiber) to maintain equal exposure levels across all experimental groups. Two packs of 3R4F research cigarettes were smoked each day, intermittently to mimic the behavior of human smokers, 5 days per week. The smoke was routed to a mixing compartment to mix with air and the mixture distributed between two exposure chambers, each containing four cages with

the materials. The gravimetric method was used to determine the total particulate matter (TPM) concentrations in each smoke chamber as previously done. The TPM values were adjusted to 30 ± 5 $\mu g/m^3$ which is within the values found by the EPA in the homes of smokers. All cigarettes were smoked and stored in accordance with the Federal Trade Commission (FTC) smoking regimen. At the end of each week, cages were removed from the exposure chamber, bagged, and transported to the vivarium where mice were placed into the cages with the THS-exposed material. Exposure was performed as previously described [6].

Protein extraction from tissues

Brain or liver tissues were collected after the appropriate exposure to THS and immediately frozen and stored at –80°C. Tissues were homogenized in radioimmunoprecipitation assay buffer (RIPA), centrifuged, and the supernatant collected for the studies unless otherwise specified by the assay procedures. All procedures described below have been performed previously by us [7] and are therefore described briefly.

Blood collection

Blood was collected directly from the heart and allowed to coagulate on ice for 20–30 min. The samples were then centrifuged at 10000 rpm for phase separation, and the serum was used immediately or frozen and stored at –80°C for future assays.

Blood glucose analysis

Fasting blood glucose levels were measured using a commercially available kit (TRUE result) and gold sensor laser accuracy strips. Mice were fasted for 12 h in order to ensure that both glucose and insulin were at the base levels. Both variables were affected by food and water and that effect varied from animal to animal. Therefore, in order to make sure that we could compare the levels of glucose and of insulin amongst animals, we always fasted mice under the same conditions. To obtain fasting blood glucose levels, a nick was made on the tail vein and the glucose levels were measured by bringing the strip into contact with the drop of blood, which then the TRUE result glucose reader provided a readout of the levels of glucose present in the blood.

Fasting serum insulin concentration

We used the ALPCO Mouse Insulin ELISA Kit (Cat# 80-INSMS-E01) and followed the protocol provided by the manufacturer. The plates were read at $\lambda = 450$ nm. Concentration of the samples was obtained from the standard curve.

HOMA-IR

Homeostatic model assessment equation (HOMA) is a method for assessing IR derived by (fasting blood glucose × fasting insulin)/22.5.

Measurement of SOD activity

We used Cayman Superoxide Dismutase Assay Kit (Cat# 706002) to measure the superoxide dismutase (SOD) levels in liver and brain tissues. SOD activity was quantitated by measuring the dismutation of superoxide radicals generated by xanthine oxidase and hypoxanthine. A standard curve was generated and used to quantitate SOD activity.

Measurements of H_2O_2 levels

We used Cayman Hydrogen Peroxide Assay Kit (Cat# 600050) to measure H_2O_2 levels in liver and brain tissues. H_2O_2 was detected using the probe 10-acetyl-3,7-dihydroxyphenoxazine (ADHP) in the presence of horseradish peroxidase, producing a highly fluorescent resorufin which was then quantitated using a spectrophotometer. A standard curve was generated to quantitate hydrogen peroxide.

Measurement of catalase activity

We used Cayman Catalase Assay Kit (Cat# 707002) to measure catalase activity in the liver and brain tissues. Catalase activity was quantitated by measuring the reaction of catalase with methanol in the presence of an optimal concentration of H_2O_2. The chromogen 4-amino-3-hydrazino-5-mercapto-1,2,4-triazole (purpald) was used to measure the reaction rate, using spectrophotometer. A standard curve was generated and used to quantitate the activity of catalase.

Clinical Science (2017) **131** 2409–2426
DOI: 10.1042/CS20171053

Measurements of GPx activity

We used Cayman GPx activity assay kit (Cat# 703102) to measure GPx (Cat# 703102) activity in the liver and brain tissues. GPx activity was quantitated by the coupled reaction of GPx with glutathione reductase (GR). GSSG, produced upon reduction of an organic hydroperoxide by GPx, was recycled to its reduced state GR and NADPH. The oxidation of NADPH to $NADP^+$ was accompanied by a decrease in absorbance at 340 nm. The rate of decrease in the A340 was directly proportional to the GPx activity in the liver and brain samples.

Measurement of DNA damage

DNA damage was measured using ELISA Kit from Cell BioLabs, Inc. (Cat# STA-320). DNA damage was quantitated by measuring levels of 8-hydroxy-2-deoxyguanosine (8-OH-dG) in brain and liver tissues. DNA was extracted from tissues as previously described [7]. A standard curve was generated and used to quantitate 8-OH-dG in the extracted brain and liver DNA.

Measurement of nitrosylation of proteins

Protein damage was quantitated by measuring the nitrosylation of tyrosine residues in proteins using ELISA Kit from Cell BioLabs (Cat# STA-305). Proteins were extracted from liver and brain samples as previously described. Samples were then loaded on to a 96-well ELISA plate precoated with anti-nitrotyrosine antibody followed by an HRP–conjugated secondary antibody. Nitrotyrosine levels were then interpolated from a standard curve.

Measurement of lipid peroxidation

Lipid peroxidation in the liver and brain tissues was determined by the levels of the by-product of lipid peroxidation known as malondialdehyde (MDA) using a kit from Cell BioLabs (Cat# STA-330). The unknown MDA containing samples or MDA standards were first reacted with thiobarbituric acid (TBA) to form what are known as TBA reactive substances which can then be quantitated by comparison with the predetermined TBARS standard curve.

Measurement of ALT levels

ALT levels were measured using ELISA Kit from Cayman Chemicals (Cat# MAK055), and quantitated by incubation of liver and serum samples in an anti-ALT antibody coated plate, followed by HRP–conjugated secondary antibody. A standard curve was generated and used to quantitate ALT in the tissue and serum.

Measurement of ATP levels

The ATP levels in liver and brain tissues were quantitated using a kit from BioVision (Cat# K354-100). ATP levels were quantitated by measuring the phosphorylation of glycerol. The product of this phosphorylation reaction was read at $\lambda = 570$ nm and the absorbance readings of the standards were used to generate a standard curve. The unknown levels of ATP in the samples were interpolated from a standard curve.

Measurement of serum cytokines

The levels of cytokines in the serum were quantitated using ELISA array kit from R&D systems (Cat# ARY006). This ELISA assay kit allowed for the analysis of multiple cytokines and chemokines simultaneously, interleukin-1α (IL-1α), MCP-1, IL-1β, IL-2, interleukin-4 (IL-4), interleukin-6 (IL-6), interleukin-10 (IL-10), IL-12, IL-17, IFN-γ, TNF-α, G-CSF, and GM-CSF. Serum was incubated in corresponding ELISA wells of each cytokine tested, incubated with the corresponding antibody, followed by HRP–conjugated secondary antibody. A standard curve was generated and used to quantitate the levels of each cytokine tested.

Measurement of serum ACTH

The adrenocorticotropic hormone (ACTH) levels in the serum were quantitated using ELISA Kit from MyBioSource (Cat# MBS52341). ACTH levels were quantitated by incubation of serum in an anti-ACTH antibody-coated plate, followed by HRP–conjugated secondary antibody. A standard curve was generated and used to quantitate ACTH levels.

Measurement of serum CRH

The corticotropin-releasing hormone (CRH) levels in the serum were quantitated using an ELISA Kit from My-BioSource (Cat# MBS16352). CRH levels were quantitated by incubation of serum in an anti-CRH antibody-coated

plate, followed by HRP–conjugated secondary antibody. A standard curve was generated and used to quantitate CRH levels.

Measurement of serum dopamine

The dopamine levels in the serum were quantitated using an ELISA Kit from MyBioSource (Cat# MBS32332). Dopamine levels were quantitated by incubation of serum in an anti-dopamine antibody-coated plate, followed by HRP–conjugated secondary antibody. A standard curve was generated and used to quantitate dopamine levels.

Measurement of serum epinephrine

The epinephrine levels in the serum were quantitated using ELISA Kit from MyBioSource (Cat# MBS12232). Epinephrine levels were quantitated by incubation of serum in an anti-epinephrine antibody-coated plate, followed by HRP–conjugated secondary antibody. A standard curve was generated and used to quantitate epinephrine levels.

Measurement of NRF1

The nuclear respiratory factor 1 (NRF1) levels in the liver were quantitated using ELISA Kit from MyBioSource (Cat# MBS1235327). NRF1 levels were quantitated by incubation of liver in an anti-NRF antibody-coated plate, followed by HRP–conjugated secondary antibody. A standard curve was generated and used to quantitate NRF1 levels.

Western blots for p38 and p-Erk

We used the procedure previously published by us [7]; for details, see the S1 Methods in [7].

Measurement of serum POMC

The proopiomelanocortin (POMC) levels in the serum were quantitated using ELISA Kit from MyBioSource (Cat# MBS1315234). POMC levels were quantitated by incubation of serum in an anti-POMC antibody-coated plate, followed by HRP–conjugated secondary antibody. A standard curve was generated and used to quantitate POMC levels.

Statistical analysis

For the statistical analysis of experiments, we used GraphPad InStat Software (GraphPad, La Jolla, CA, U.S.A.). Statistical comparisons between two groups was performed using the unpaired Student's t test. We also used a 2×3 ANOVA comparing the effects of treatment (THS or control) with time (2, 4, and 6 months). All data are mean $\pm$ S.D. represented by the error bars. Means were considered significantly different when $P<0.05$.

Results

For all the studies shown here, we investigated levels of various molecules chosen to detect liver and brain damage as well as metabolic syndrome markers. We exposed different cohorts of mice to THS for 2, 4, and 6 months and tested these mice against 24 biomarkers (Table 1). Fifteen biomarkers were tested in serum and nine biomarkers were tested in liver and brain tissue of the mice exposed to THS in a time-dependent manner. For those variables that showed increases at 2 months of exposure, we then determined if they were already altered at 1 month of exposure.

The data are presented in four sections: effects on insulin metabolism, on oxidative stress, on hormonal changes, and on inflammation. Fasting blood glucose and insulin were used to test for metabolic syndrome. H_2O_2, SOD, catalase, GPx, nitrotyrosine, lipid peroxidation, and DNA damage were used to test for liver and brain oxidative stress. CRH, ACTH, epinephrine, and cortisol were used to test for hormonal alterations. IL-1α, IL-4, IL-6, IL-10, GM-CSF, and TNF-α were used to test for markers of inflammation.

Time required for THS exposure to cause hyperglycemia and insulinemia

In order to determine whether there is a time-dependent increase in markers of IR with increased THS exposure and at what length of exposure the body becomes insulin resistant, we tested fasting blood glucose and insulin levels in the exposed mice. We first fasted the mice for 12 h and then obtained blood from a nick in the tail to determine the blood glucose levels. The mice were then killed and blood obtained from the heart to test for insulin levels. We found that fasting blood glucose and serum insulin levels increased after 3–4 months of THS exposure (Figure 1A,B). To quantitate IR, we used the homeostatic IR index (HOMA-IR) and found that mice exposed to THS for 4 and 6 months had significantly higher indices than controls (Figure 1C). At 2 months, we begin to see the general trend that fasting blood glucose and insulin levels are increasing. However, it takes the body approximately 3–4 months for the differences to become significant.

PORTLAND PRESS

Clinical Science (2017) **131** 2409–2426
DOI: 10.1042/CS20171053

Table 1 Biomarkers examined to test the damage caused by THS exposure over time

Biomarkers	Detecting material
Fasting blood glucose	Serum
Insulin	Serum
CRH	Serum
ACTH	Serum
Epinephrine	Serum
Cortisol	Serum
POMC	Serum
Dopamine	Serum
IL-1α	Serum
IL-4	Serum
IL-6	Serum
IL-10	Serum
GM-CSF	Serum
TNF-α	Serum
Aspartate aminotransferase (AST)	Serum
Urea	Serum
H_2O_2	Liver; brain
SOD	Liver; brain
Catalase	Liver; brain
GPx	Liver; brain
Nitrotyrosine	Liver; brain
Lipid peroxidation	Liver; brain
DNA damage	Liver; brain
ATP	Liver; brain
Lactate	Liver; brain
NRF	Liver
POMC	Brain

Fifteen biomarkers were tested in serum, nine biomarkers were tested in liver and brain tissue.

Time required for THS exposure to cause oxidative stress

Cigarette smoke toxins, such as those found in THS, are potent sources of reactive oxygen species (ROS) [17]. To determine whether mice exposed to THS have oxidative stress in the liver, the organ that detoxifies the body, we measured the levels of H_2O_2 and found that by 2 months of exposure, H_2O_2 was already significantly increased in the liver tissue of THS-exposed mice (Figure 2A). Because H_2O_2 is produced by SOD we measured the activity of this enzyme to determine whether it is also elevated. Indeed, we found that SOD was significantly increased by 2 months (Figure 2B), much like H_2O_2. H_2O_2 is a reactive molecule and therefore needs to be quickly broken down to H_2O and O_2 by catalase and GPx, two antioxidant enzymes, before it damages the cells. However, catalase activity was the same as in control at 2 months, but by 4–6 months the activity of this enzyme was significantly decreased (Figure 2C). GPx activity was also not significantly changed earlier but it decreased at 6 months (Figure 2D). Taken together, these results show that THS exposure reduces the antioxidant potential of the liver and leads to increased oxidative stress. Furthermore, the increased levels of H_2O_2 can react with Fe^{2+} ions in the tissue and undergo the Fenton reaction leading to production of hydroxyl radicals [18-21]. These, in turn, can lead to protein modification, formation of DNA adducts, and lipid peroxidation. We found that THS exposure causes nitrotyrosine modification in proteins by 2 months of exposure (Figure 2E) and DNA adduct formation by 3–4 months (Figure 2F). Lipid peroxidation was not seen until 6 months of exposure (Figure 2G). Because of these molecular changes, we examined the possibility that these alterations could impair mitochondrial function by measuring the levels of ATP produced, given that ATP is the energy currency of the cell. We found that by 2 months, the levels of ATP were already significantly lower than the control (Figure 3A) and that there was a concomitant increase in lactate levels (Figure 3B), suggesting a switch in energy production from oxidative phosphorylation to glycolysis. We also measured two other biomarkers that indicate liver malfunction when elevated, aspartate aminotransferase (AST) and urea. Both were elevated by 2 months of exposure (Figure 3C,D). Given that there is an increased oxidative stress, molecular damage, as well as mitochondrial dysfunction in the liver, we examined the levels of NRF1, a nuclear transcription factor that becomes

Clinical Science (2017) **131** 2409–2426
DOI: 10.1042/CS20171053

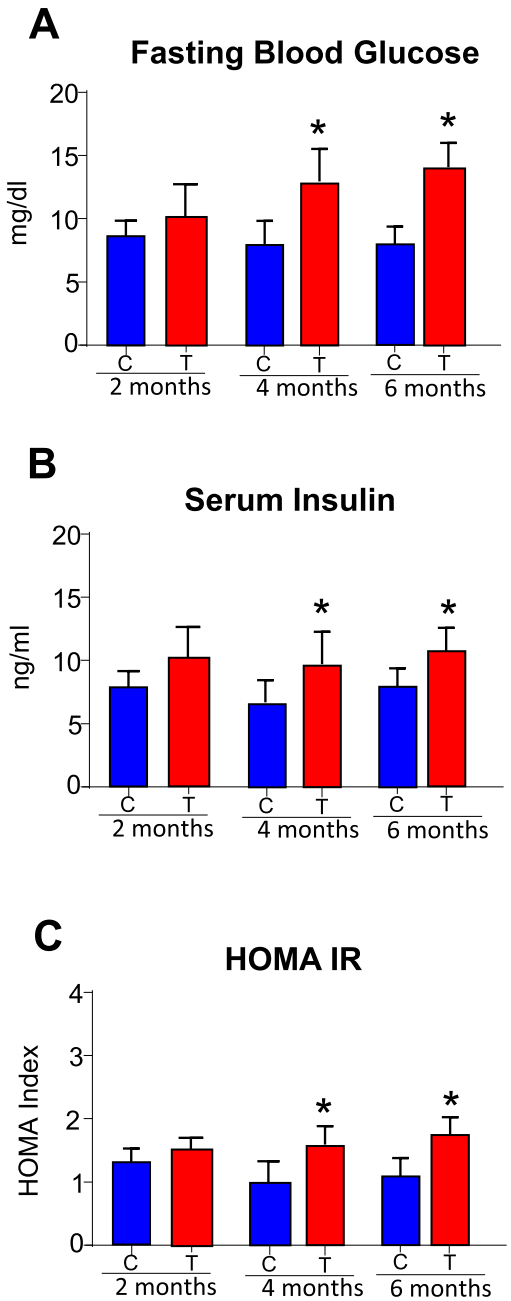

Figure 1. Increased time of exposure to THS stimulates hyperglycemia and insulinemia in a time-dependent manner

THS exposure results in (**A**) increased fasting glucose levels at 4 months, (**B**) increased fasting insulin levels at 4 months, and (**C**) increased HOMA-IR index (fasting blood glucose × fasting insulin/22.5) at 4 months of exposure. All data are expressed mean ± S.D.; *$P<0.05$, $n=9$. *P*-values were adjusted for the number of times each test was run.

up-regulated, in the liver, in response to oxidative stress or inflammation. We found that in the liver of 2 months old THS-exposed mice, NRF1 levels were much higher than in controls (Figure 3E), suggesting that as early as 2 months of exposure to THS, the body is under significant oxidative stress, however NRF1 is failing to combat this oxidative stress because that oxidative stress continues to see it worsen as time of exposure increases.

Because we have previously shown that THS exposure affects behavior, we measured the levels of H_2O_2 as well as the levels of SOD and catalase and GPx activity in brain tissue. H_2O_2 levels increased significantly by 4 months of THS exposure (Figure 4A). Interestingly, we did not observe a significant increase in SOD activity in the brain (Figure 4B) as we did in the liver, and catalase and GPx activities were only significantly decreased by 6 months after THS exposure

Clinical Science (2017) 131 2409–2426
DOI: 10.1042/CS20171053

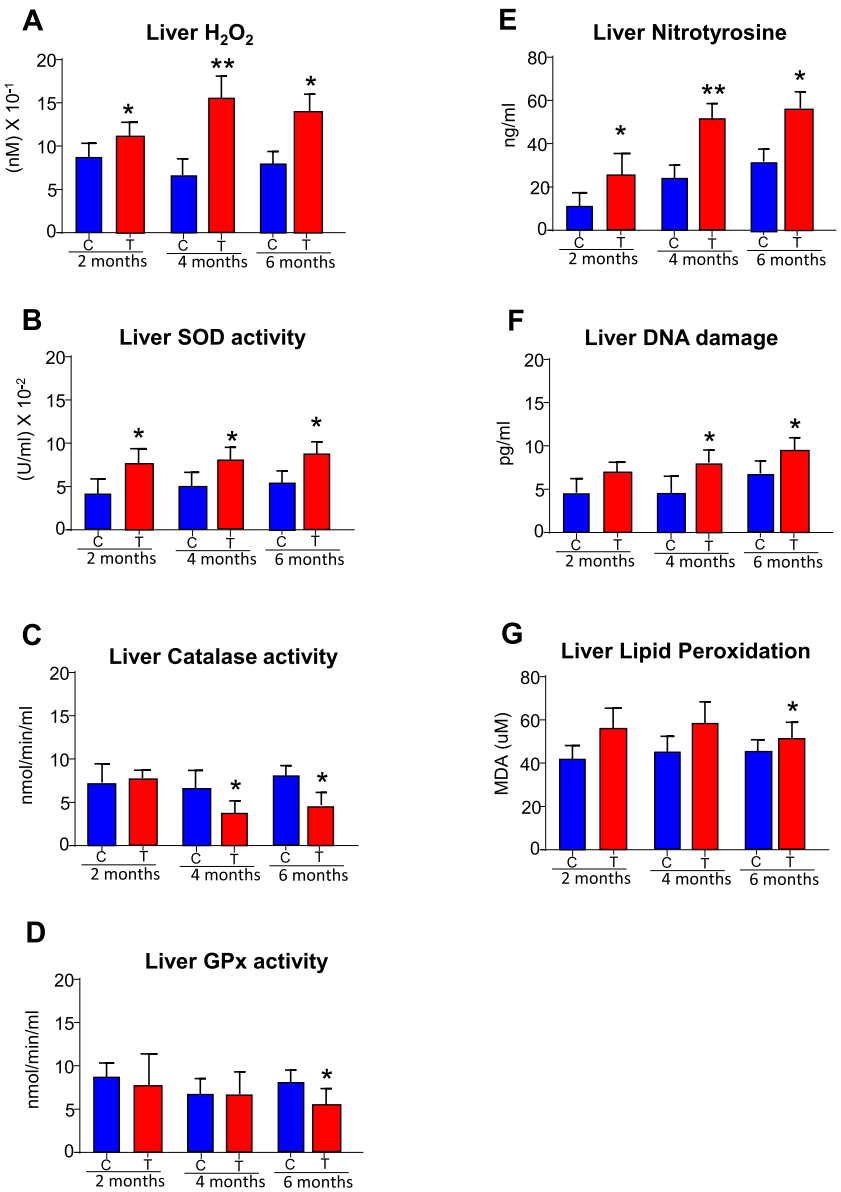

Figure 2. THS induces oxidative stress and oxidative stress mediated damage in the liver in a time-dependent manner

THS exposure results in (**A**) higher levels of hepatic H_2O_2 starting at 2 months of exposure, (**B**) higher SOD activities starting at 2 months of exposure, (**C**) lower catalase enzymatic activity at 4 months of exposure, (**D**) lower GPx enzymatic activity at 6 months of exposure, (**E**) higher levels of nitrotyrosine at 2 months of exposure, (**F**) higher DNA damage at 4 months of exposure, (**G**) and higher lipid peroxidation after 6 months of exposure in a time-dependent manner. All data are expressed mean ± S.D.; *$P<0.05$, $n=9$. P-values were adjusted for the number of times each test was run.

(Figure 4C,D). We also observed oxidative stress mediated molecular damage in the brain of THS-exposed mice with significantly elevated levels of nitrotyrosine that occurred in 2 months of THS exposure (Figure 4E). However, DNA damage (Figure 4F) and lipid peroxidation (Figure 4G) were not seen until 6 months of THS exposure. The differences in the findings between brain and liver suggest that the brain might have less oxidative stress due to THS exposure because the blood–brain barrier might play a protective role regarding the THS toxins.

Given that we observed molecular damage in the brain, we examined the levels of ATP production and found that by 2 months of THS exposure, mice had decreased ATP production (Figure 5A). This decrease was accompanied by an increase in lactate (Figure 5B) much like we observed in the liver, indicating a switch to glycolysis as an alternative way for energy production.

Clinical Science (2017) **131** 2409–2426
DOI: 10.1042/CS20171053

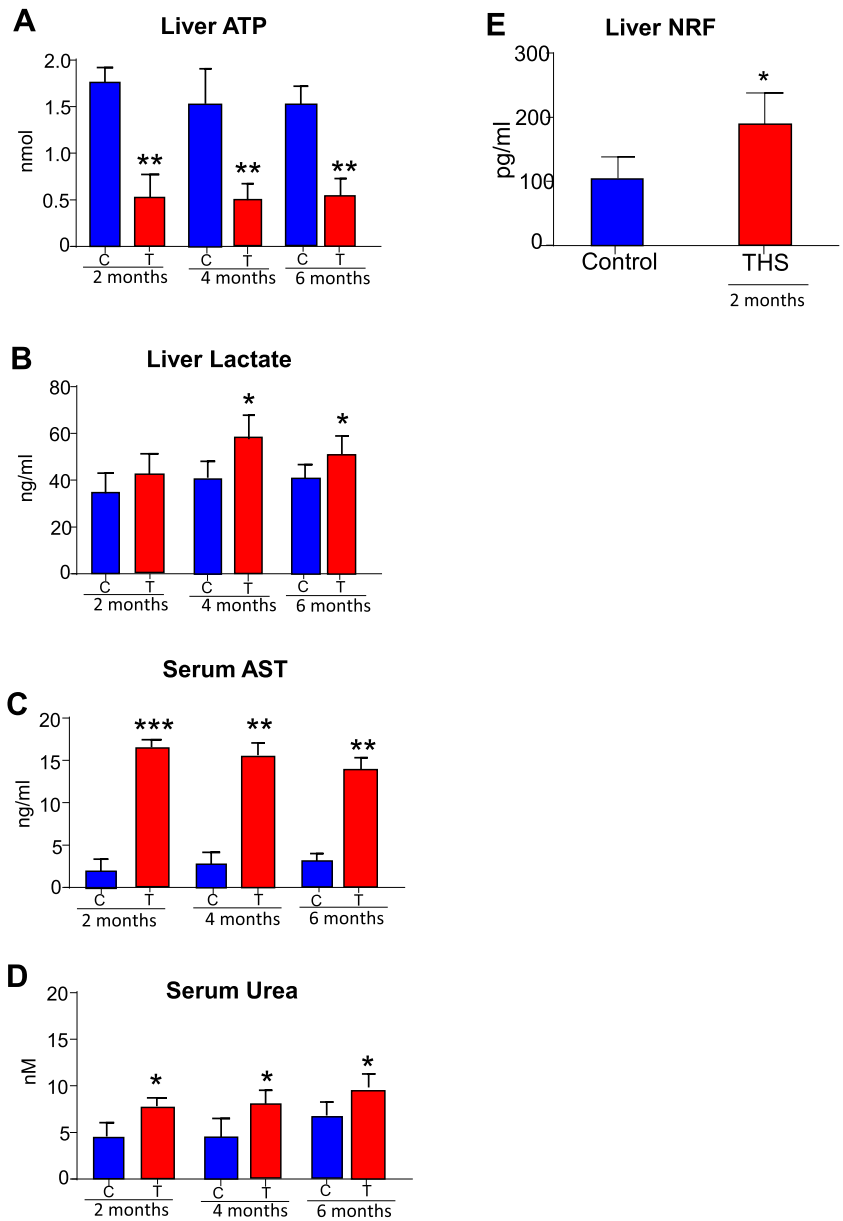

Figure 3. Time-dependent exposure to THS results in mitochondrial dysfunction and damage to the liver

THS-exposed mice produce (**A**) lower levels of ATP at 2 months of exposure, (**B**) higher levels of lactate at 4 months of exposure, (**C**) higher levels of serum AST starting at 2 months of exposure, and (**D**) higher levels of serum urea at 2 months of exposure. (**E**) Two months of THS exposure results in an increase in NRF1 in the liver, a factor is elevated when oxidative stress and inflammation are high. All data are expressed as mean ± S.D.; *P<0.05, **P<0.01; n=9. P-values were adjusted for the number of times each test was run.

Time required for THS exposure to cause hormonal alterations

During times of physiological stress (e.g. THS toxins), the body activates the hypothalamus–pituitary axis (HPA axis), a complex set of neuroendocrine-mediated changes that regulates many body processes, including insulin sensitivity, the immune system, mood, energy storage/expenditure, and physically prepares the body to combat stressors [22-24]. Upon detection of stress by the brain, the hypothalamus secretes a hormone known as CRH which then stimulates the anterior pituitary to release ACTH which, in turn, travels in the blood to the adrenal glands to stimulate the secretion of hormones such as cortisol and epinephrine which are stress responders. We observed that CRH was only significantly more elevated at 6 months of exposure (Figure 6A) whereas ACTH was elevated as early as 2 months (Figure 6B). Similarly, epinephrine was increased by 2 months of exposure (Figure 6C) but cortisol was only seen to

PORTLAND PRESS

Clinical Science (2017) **131** 2409–2426
DOI: 10.1042/CS20171053

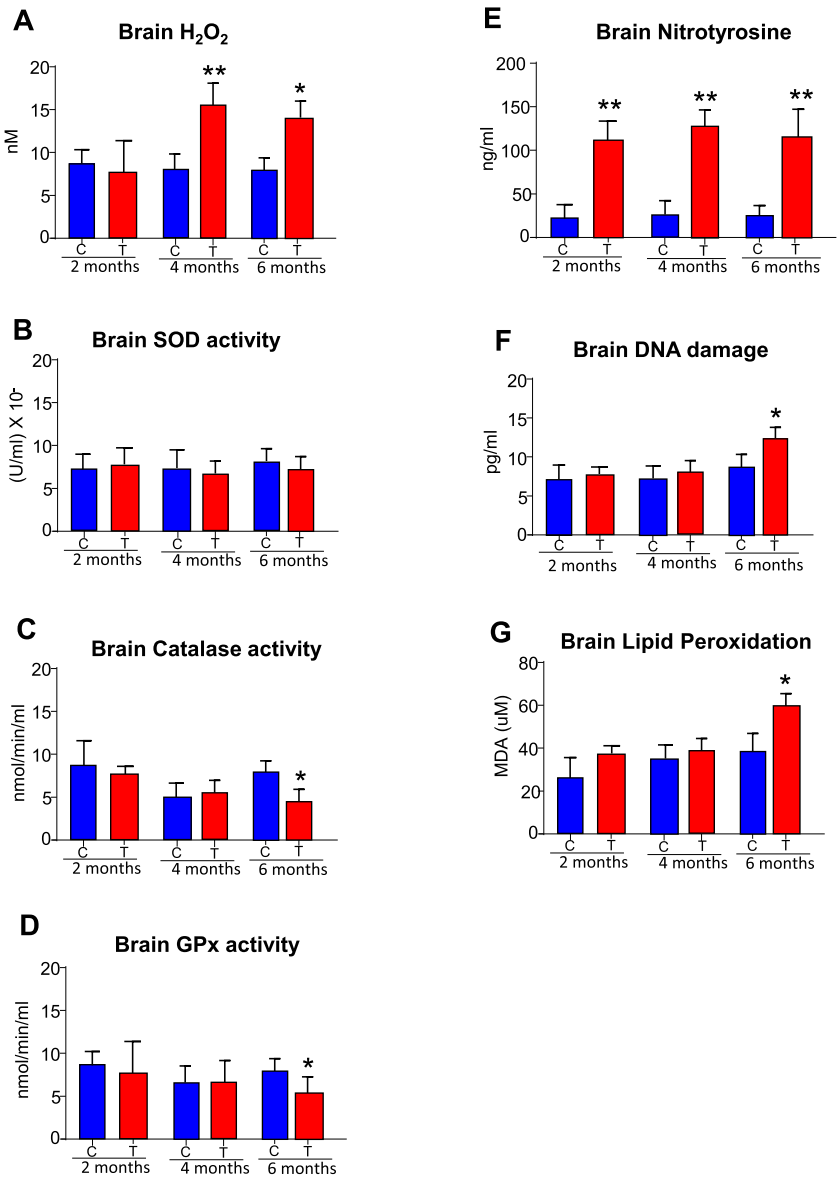

Figure 4. THS induces oxidative stress and oxidative stress mediated molecular damage in the brain

THS-exposed mice have higher levels of H_2O_2 at 4 months of exposure (**A**), normal levels of SOD activity, (**B**) but lower levels of catalase activity at 6 months, (**C**) lower GPx enzymatic activity at 6 months, (**D**) higher levels of nitrotyrosine at 2 months of exposure (**E**), higher levels of DNA damage at 6 months of exposure (**F**), and higher levels of lipid peroxidation at 6 months of exposure (**G**). All data are expressed as mean ± S.D.; *P<0.05, n=9. P-values were adjusted for the number of times each test was run.

be elevated at 4 months of exposure (Figure 6D). Given the fact that ACTH was increased independently from CRH levels, we determined whether this was due to the increased production of the POMC hormone. This hormone is involved in an alternative pathway of ACTH production. During times of oxidative stress in the brain, the hypothalamus gland will secrete POMC hormone, which will activate the pituitary gland to produce ACTH [25]. We found that, both in the serum and brain of mice exposed to THS for 2 months, there were increased levels of the POMC hormone (Figure 6E,F).

Time required for THS exposure to increase markers of inflammation

In order to determine whether exposure to THS toxins results in an increase in inflammation in a time-dependent manner, we examined the levels of cytokines in the serum. We found several proinflammatory cytokines were elevated

Clinical Science (2017) **131** 2409–2426
DOI: 10.1042/CS20171053

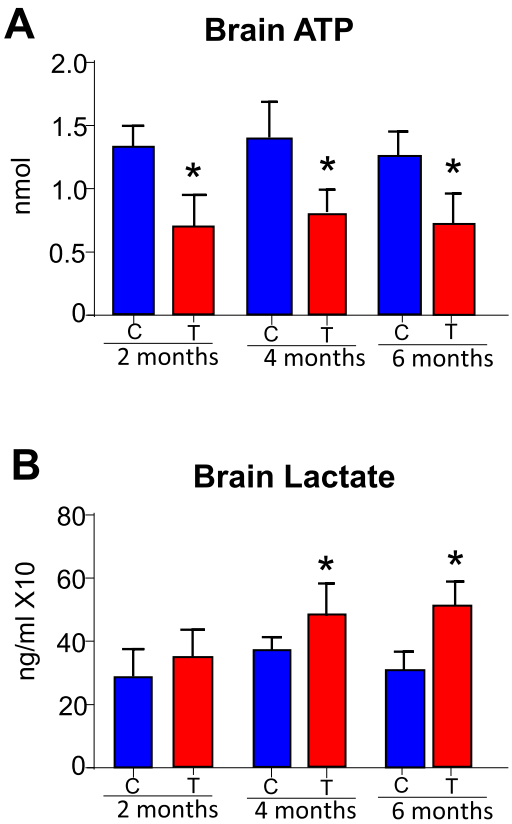

Figure 5. Increased time of THS exposure results in mitochondrial dysfunction in the brain

THS-exposed mice, have lower levels of ATP at 2 months of exposure (**A**), and higher levels of lactate at 4 months of exposure (**B**). All data are expressed as mean ± S.D.; *$P<0.05$, $n=9$. P-values were adjusted for the number of times each test was run.

(for a list of cytokines in the array, see the Materials and methods section). Mice exposed to THS for as early as 2 months had the proinflammatory cytokines IL-1α, IL-6, GM-CSF, and TNF-α levels significantly higher than those of the controls (Figure 7A–D). Collectively these cytokines indicate a proinflammatory condition in response to THS exposure. THS-exposed mice also have increased anti-inflammatory cytokines IL-4 and IL-10 (Figure 7E,F). These data taken together show that as early as 2 months, THS-exposed mice suffer from significant inflammation. Because it is known that pathways involved in inflammatory responses that are driven by cytokines commonly involve the mitogen-activated protein kinases, P38 and ERK [26-28], we determined whether these kinases are involved in the THS-induced inflammatory response. We found that P38 levels were increased in the liver of mice exposed to THS for 2 months and so were the levels of p-ERK, which is the form of functional ERK (Figure 7G,H).

THS exposure and the resulting cellular damage after one-month of exposure

To determine whether the biomarkers that were altered at 2 months after THS exposure were already altered at 1 month of exposure, the mice were exposed to THS for only 1 month, and the biomarkers that we tested and showed significance at 2 months were examined at 1 month. These biomarkers included serum ACTH, epinephrine, AST, and urea, nitrosylation of proteins in the liver and brain, and the proinflammatory cytokines, IL-1α, IL-4, IL-10, GM-CSF, and TNF-α. We found that 1 month of THS exposure resulted in significant increases in, epinephrine, TNF-α, GM-CSF, and serum AST but not the other markers. (Figure 8A–H).

Discussion

The goal of the present study was to determine the minimum amount of time required to cause physiological changes in mice when they are exposed to THS, using an exposure system that mimics human exposure. In order to verify that THS exposure over time had a significant difference in the changes to the variables we measured, we used a mixed

Clinical Science (2017) **131** 2409–2426
DOI: 10.1042/CS20171053

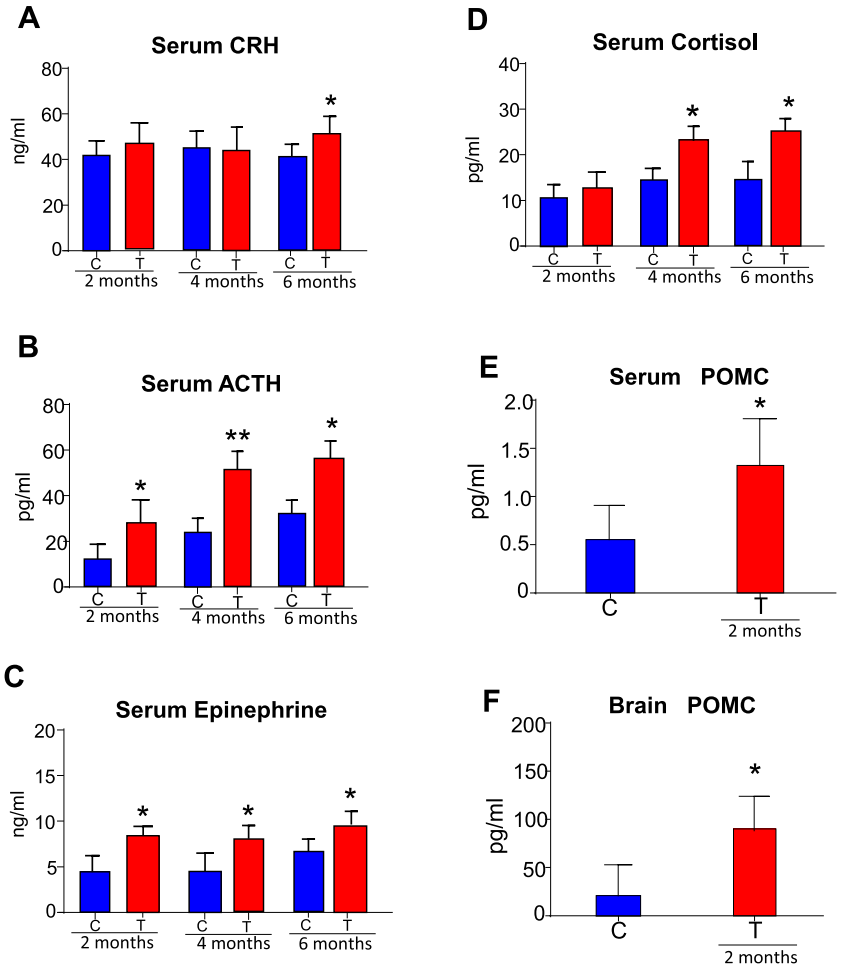

Figure 6. Increased time of THS exposure results in alterations in the levels of hormones involved in stress response and metabolism

THS-exposed mice show (**A**) increased CRH levels in the serum at 6 months of exposure, (**B**) increased ACTH levels at 2 months of exposure, (**C**) increased epinephrine levels at 2 months of exposure, (**D**) increased cortisol levels at 4 months of exposure, (**E**) increased serum POMC, and (**F**) increased POMC levels in the brain, which activates ACTH secretion. All data are expressed as mean ± S.D.; *$P < 0.05$, $n=9$. *P*-values were adjusted for the number of times each test was run.

model repeated measure two-ANOVA to determine whether the effects of THS are dependent on exposure time and we found a positive time-dependent significant correlation with increase time of THS exposure and the effects it had on all the variables we measured. Figure 9 shows that of the biomarkers tested, the ones altered in the serum after only 1 month of THS exposure are GM-CSF, TNF-α, epinephrine, and AST and that in the liver and brain tissues we have increased nitrotyrosine levels. In addition to continued alteration in the biomarkers we found to be changed at 1 month, after 2 months of exposure, we found increased fasting blood glucose and IL-6 in the serum. In the liver, we find increased hydrogen peroxide levels and increased SOD activity but decreased catalase activity, as well as increased DNA damage. At this time of exposure in the brain, we find increased hydrogen peroxide levels. After 4 and 6 months of exposure, we also find increased serum insulin and CRH levels. We also show molecular alterations to pathways of oxidative stress response through increased presence of NRF1, stress hormone production pathways through POMC, and inflammatory response pathways through P38, and ERK. Our studies can indicate whether or not, and for how long, a mouse has been exposed to THS, by measuring these variables in the blood, making these biomarkers both easy to test and highly correlative with THS exposure.

In our previous research, we observe that mice exposed to THS for 6 months, develop symptoms of IR and metabolic syndrome, with increases in fasting blood glucose, fasting serum insulin, and HOMA-IR index [7]. In the studies presented here, we show that there is an increase in biomarkers of IR with increased THS exposure, as well as

Clinical Science (2017) **131** 2409–2426
DOI: 10.1042/CS20171053

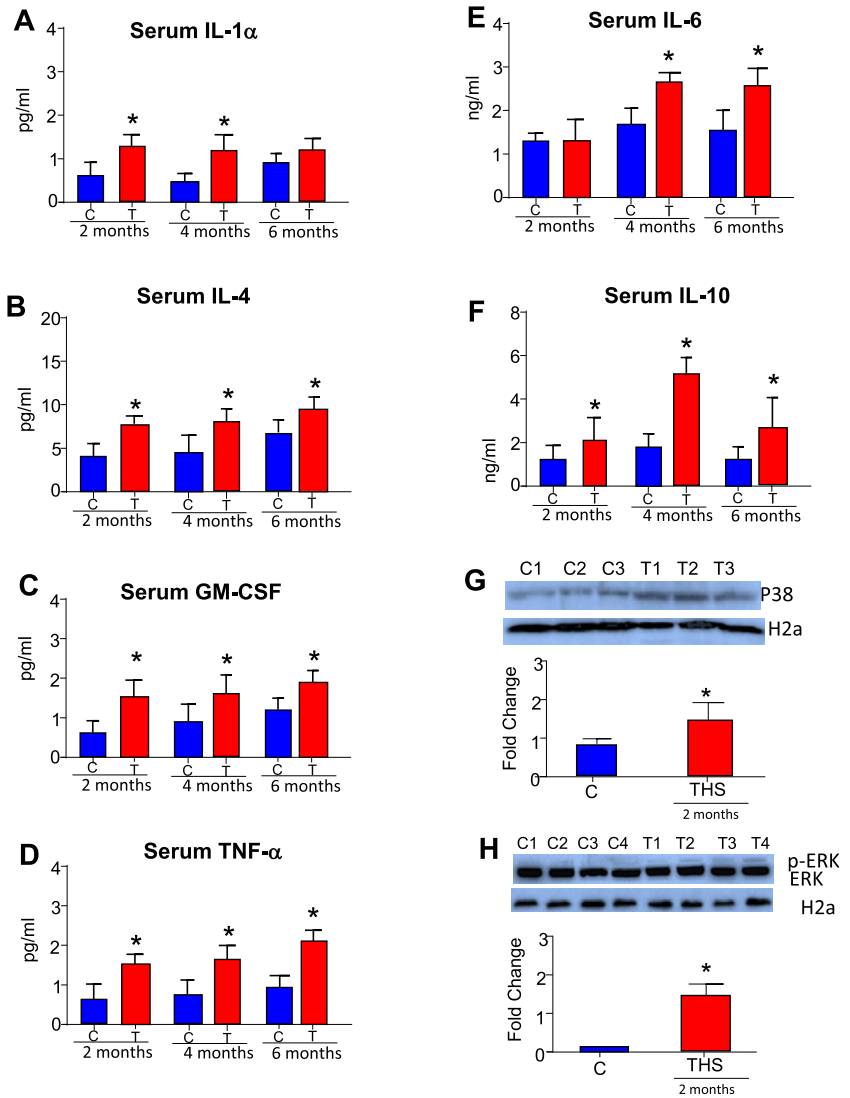

Figure 7. Exposure to THS over time results in systemic inflammation

When compared with the controls, in the serum of THS-exposed mice there is an increase at 2 months of exposure of (**A**) IL-1α, (**B**) IL-4, (**C**) GM-CSF, (**D**) TNF-α, (**E**) IL-6 levels at 4 months of exposure, and (**F**) IL-10 levels at 2 months of exposure. (**G**) In the liver at 2 months of exposure to THS, there is increased P38 levels and (**H**) an increase in p-ERK levels. All data are expressed as mean ± S.D.; **P*<0.05, *n*=9. *P*-values were adjusted for the number of times each test was run.

identifying critical times of exposure at which the body becomes insulin resistant. Fasting blood glucose, serum insulin, and the HOMA-IR index were increased in a time-dependent manner with THS exposure, showing that as early as 4 months of THS exposure, the animals already have a propensity for type 2 diabetes. In humans, small increases in blood glucose, over time, are highly damaging to the blood vessels and other tissues [29]. Formation of glycation end products on proteins present in cell membranes have been associated with increased blood glucose levels and have been one of the leading causes of cardiovascular diseases [30].

We have reported in previous studies the development of oxidative stress in multiple organs, including the lung, liver, skeletal muscle, brain, adrenal, and skin, after 6 months of THS exposure [6-9]. The work presented here focusses on the liver and brain because the liver plays a major role in metabolism and detoxification, and the brain also plays significant roles in behavior.

In the liver, the data we obtained on the oxidative stress levels after THS exposure show increases in H_2O_2 levels and SOD activity as early as 2 months. SOD is the primary enzymatic defense in the liver against the damaging effects of $O_2^{\bullet-}$, by converting $O_2^{\bullet-}$ into H_2O_2 which is a substrate for catalase and GPx [31]. Because catalase and

Clinical Science (2017) **131** 2409–2426
DOI: 10.1042/CS20171053

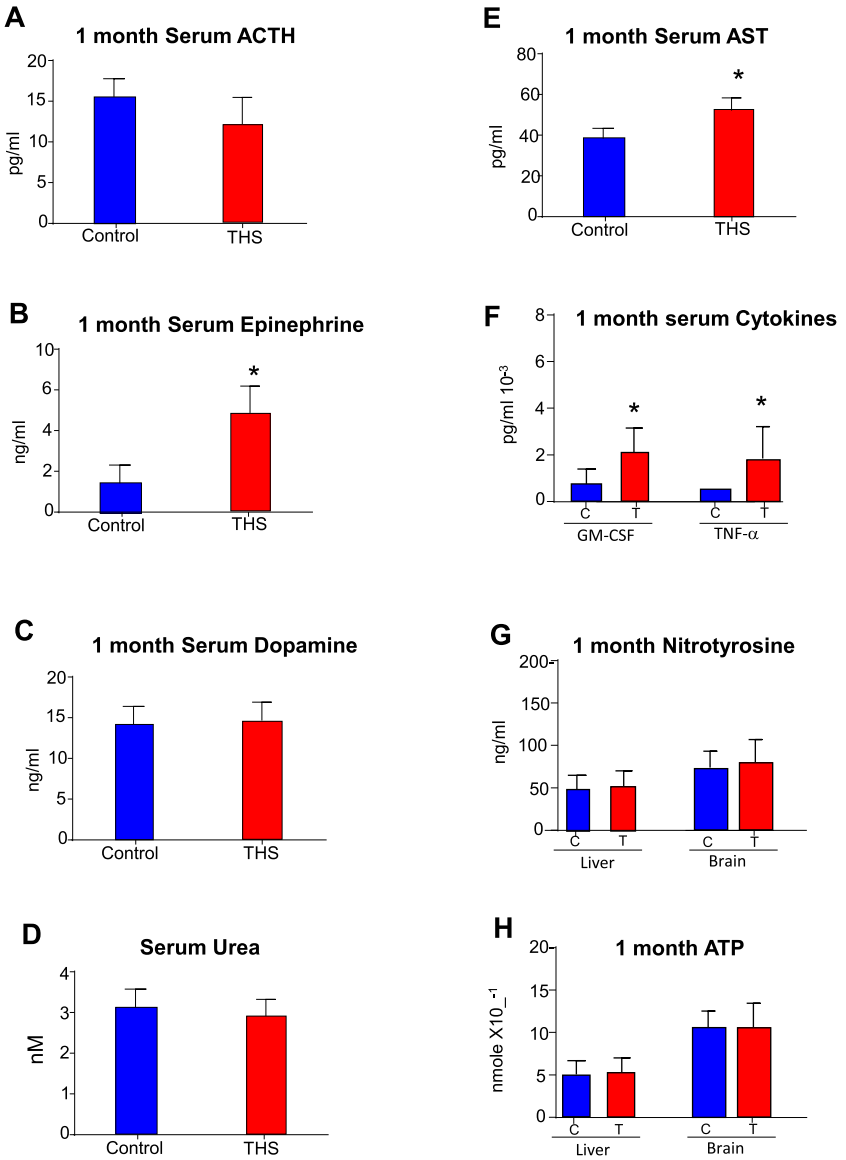

Figure 8. Exposure to THS for 1 month results in early damage

One month THS-exposed mice show (**A**) no significant difference in serum ACTH levels, (**B**) higher serum epinephrine levels, (**C**) equivalent serum levels of dopamine, (**D**) equivalent serum urea levels, (**E**) higher serum AST levels, (**F**) higher serum cytokines (GM-CSF and TNF-α) levels (**G**) equivalent tissue nitrotyrosine levels, and (**H**) equivalent tissue ATP levels. All data are expressed as mean ± S.D.; *P<0.05, n=9. P-values were adjusted for the number of times each test was run.

GPx activity levels are unchanged in the THS-exposed mice, H_2O_2 is not broken to H_2O and $O_2^{\bullet}$. Under these conditions, H_2O_2 participates in the Fenton reaction leading to OH radicals, which are damaging to proteins, lipids, and DNA. The implications of this damage in an organ such as the liver is significant because it can hinder the capability of the organ to detoxify the body, leading to more exacerbated damage by THS toxins. Nitrotyrosine is widely used as a marker of post-translational modification by the nitric oxide ($^{\bullet}$NO, nitrogen monoxide) derived oxidant peroxynitrite ($ONOO^{\bullet-}$), formed when ROS are not effectively cleared by the natural antioxidant defense systems and as a result can react with proteins in the cell, nitrating them which potentially changes functionality, and as a result, compromises tissue function [32]. We observe high levels of nitrated proteins as early as 2 months of THS exposure, which can show how sensitive the liver is to these toxins and how ineffective it becomes to clear these ROS when exposure to THS occurs. Hydroxyl radicals react with DNA and, as a result, lead to the formation of adducts

Clinical Science (2017) **131** 2409–2426
DOI: 10.1042/CS20171053

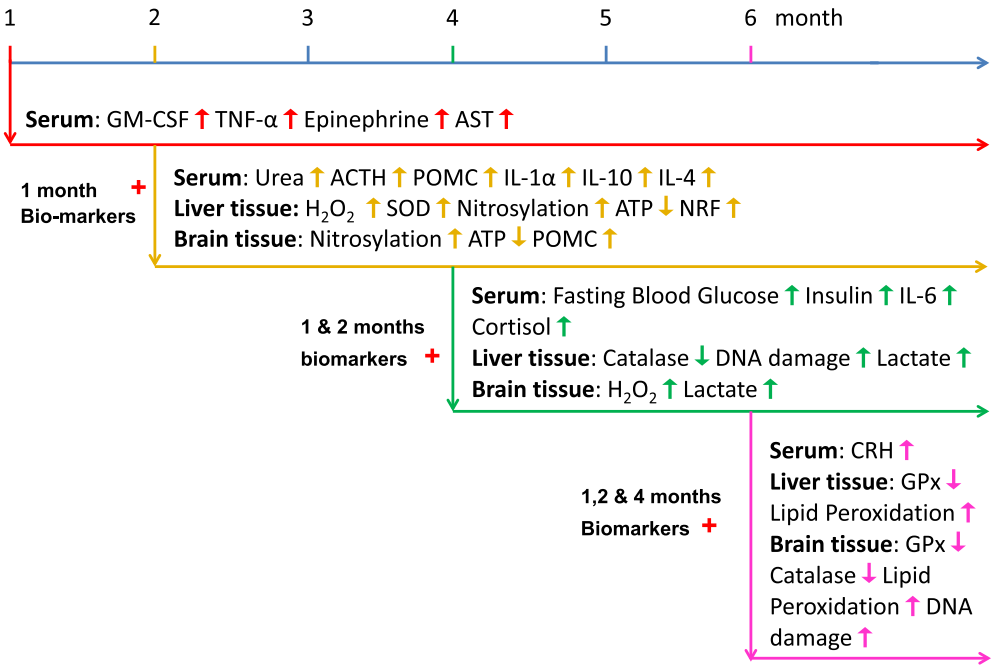

Figure 9. Summary of all of the biomarkers we found altered in response to length of THS exposure

on the DNA bases, most commonly in the form of modified 8-OH-dG, which has been shown to cause misreading of DNA during replication and affects the activity of DNA polymerase [33]. Our data show that THS exposure results in DNA damage as early as 2 months exposure, and this risk becomes significant compared with controls after 4 and 6 months of exposure. In addition, cell membranes can be modified by lipid peroxidation products, such as *trans*-4-hydroxy-2-nonenal (HNE), 4-hydroperoxy-2-nonenal (HPNE), and MDA [34]. Lipid peroxidation products can also modulate signaling molecules and alter functions of enzymes and proteins in the cell. Our data show that significant lipid peroxidation occurs by 6 months of exposure, indicating that there is a longer length of time required for damage to lipid components of cells. Taken together, these data reveal that THS exposure results in oxidative stress mediated damage which can result in the development of chronic liver diseases such as NAFLD. Protein nitrosylation and lipid peroxidation have been associated with smoke induced development of NAFLD in rodents and humans and our results are showing a time-dependent correlation with THS exposure and on set of fatty liver disease.

In the brain, we observe that it takes much longer for THS exposure to result in the accumulation of H_2O_2 and alteration in the activity of the antioxidant enzymes. We propose that this delay is due to the presence of the blood–brain barrier preventing the THS toxins from entering the tissue freely. However, we see that by 4 months, H_2O_2 levels are significantly high, and that the activity of SOD, catalase, and GPx, are reduced. In the brain we again observe the increase in nitrosylation of proteins as early as 2 months as well as increased lipid peroxidation and DNA damage by 6 months of THS exposure. Thus, compared with the brain, the liver is more susceptible to oxidative stress mediated damage.

We previously showed that mice exposed to THS for 6 months showed increased hyperactivity, stress, and anxiety, compared with their control counterparts [6]. We hypothesized that these behavioral changes caused by THS exposure might be detected early by testing for increases in stress hormones in the serum. We found that the major hormones of the hypothalamus, pituitary, adrenal stress axis (HPA), and their precursors were significantly altered in THS-exposed mice. This finding was significant not only because increases in these hormones are associated with the behavioral changes we detected, but also because these hormones have a secondary effect on insulin signaling and metabolism [35]. During times of stress, the body, through the release of epinephrine and cortisol, converts the stress signals received by the brain to physiological responses by binding to receptors in tissues such as the liver and skeletal muscle [36]. We attributed the potential role of these hormones as one of the mechanisms by which THS-exposed mice develop IR. In these studies, we determined whether these hormones are altered in a time-dependent manner and at what time point of THS exposure do these alterations occur.

Clinical Science (2017) **131** 2409–2426
DOI: 10.1042/CS20171053

Table 2 Critical serum biological biomarkers of THS exposure over time*

Early stage (≥1 month)	Middle stage (≥2 months)	Late stage (≥4 months)	Very late stage (≥6 months)
GM-CSF	ACTH	Fasting blood glucose	CRH
TNF-α	Urea	Insulin	
Epinephrine	POMC	IL-6	
AST	IL-1α, IL-4, IL10	Cortisol	

*Each column presents biological biomarkers that first appear at the labeled stage. In addition, each stage displays all of the markers in the previous stage(s).

In the present work, the HPA-axis signaling cascade hormones CRH, ACTH, cortisol, and epinephrine increased in a time-dependent manner, with epinephrine and ACTH being high as early as 2 months of THS exposure. Cortisol showed significant increases at 4 months of exposure. We noticed, however, that CRH only increased at 6 months of exposure. At 2 months of THS exposure in the brain and serum there were increased levels of POMC, which probably explains why ACTH is so high at 2 months of exposure, independent of CRH levels. Further evidence comes from the fact that at 6 months of exposure when CRH levels are high, the ACTH levels are also increased, most likely to be because ACTH is also stimulated by CRH.

We found that as early as 2 months the proinflammatory cytokines, IL-1α, IL-4, GM-CSF, and TNF-α were increased compared with controls. IL-1α is a cytokine that is increased during states of inflammation and has roles in furthering the inflammatory response by increasing production of other cytokines such as TNF-α. We see that in mice exposed to THS for 2, 4, and 6 months, the levels of IL-1α increases which indicates that these mice are in a proinflammatory state which then is further increased by the production of other cytokines. Increases in levels of IL-1α have also been shown to have negative roles in lipid and glucose metabolism pathways, both of which occur in our THS-exposed mice [37].

GM-CSF is a cytokine that is increased during states of inflammation and has roles in monocyte recruitment and stimulation, which then go into circulation, invade tissues, and become macrophages, which in turn secrete inflammatory cytokines [37]. Furthermore, GM-CSF has been shown to be a signal transducer and transcription activator in macrophages, which leads to their production of ROS as a conserved mechanism for fighting infection. GM-CSF levels are increased in THS-exposed mice as early as 2 months adding to the evidence that these mice are in a proinflammatory condition and further explaining the high amounts of ROS and oxidative stress in the tissues.

TNF-α is a cell cytokine involved in systemic inflammation, and is mostly produced by macrophages which are activated to do so by IL-1α. TNF-α has many downstream pathways most of which induce cell death, mitochondrial fission, and/or breakdown, as well as activating the p38 and ERK inflammatory pathways [38]. We found that as early as 1 month of THS exposure TNF-α levels were increased, not only indicating inflammation, cell damage, and death, but also potentially explaining mitochondrial dysfunction that we observe with THS exposure. In addition to the increase in the levels of these inflammatory cytokines, we also see anti-inflammatory cytokines such as IL-4 and IL-10 [39] increased in THS-exposed mice as early as 2 months of exposure, as the body attempts unsuccessfully to resist the inflammation caused by THS exposure.

In *summary*, we show that THS toxins have major effects on the liver and brain, and on circulating hormones and cytokines, which show the general trend of increased susceptibility of the body to metabolic diseases and inflammation as the time of THS exposure increases. These results could potentially be used to estimate the length of exposure to THS. Furthermore, these data may be important to inform the public, in particular the parents of children living in the homes of smokers, about the danger of exposure to THS. We summarize in Table 2, a key set of easily testable serum biomarkers altered as a result of THS exposure at different times. We can see that at 1 month of exposure, which we label as 'mild exposure', we detect alterations in GM-CSF, TNF-α, epinephrine, AST. 'Moderate exposure' takes ∼2 months and consists of increased ACTH, urea, POMC, IL-1α, IL-10, IL-4 in the serum. After 4 months of exposure, 'high exposure', we detect fasting blood glucose, insulin, IL-6, CRH, and cortisol in the serum. These biomarkers can potentially be used to classify how long one has been exposed to THS toxins and the extent of cellular and molecular damage that could lead to disease. Maturation of humans is much slower than in mice, hence we expect that the exposure times shown here would be longer for each stage.

Clinical perspectives

- The present study investigates the time-dependent effects of THS exposure on health, with the goal of correlating exposure time with a specific set of biomarkers.
- We showed THS exposure as early as 1 month, can lead to changes in markers of health in the serum, liver, and brain tissues. These markers increase in a time-dependent manner showing that the body has symptoms of metabolic syndrome, oxidative stress mediated cellular damage, and systemic inflammation, which progressively worsen with increased time of exposure to THS.
- Our findings will help identify the approximate length of exposure to THS as well as the extent of damage. They also provide insight into the mechanisms by which THS exposure leads to physiological changes that lead to the onset of disease. This is particularly important for children and the elderly who are sensitive bystanders exposed to THS.

Funding
This work was funded by Tobacco Research Disease Related Program (TRDRP) grants under projects 22RT-0121and 23DT-0103. The funders had no role in study design, data collection and analysis, decision to publish, or preparation of the manuscript.

Competing interests
The authors declare that there are no competing interests associated with the manuscript.

Author contribution
N.A., Y.C. and M.M.G. conceived and designed the experiments. N.A. and Y.C. performed the experiments. N.A., Y.C. and M.M.G. analyzed the data. M.M.G. contributed reagents/materials/analysis tools. N.A., Y.C. and M.M.G. wrote the paper.

Abbreviations
ACTH, adrenocorticotropic hormone; ALT, alanine aminotransferase; AST , aspartate; CRH, corticotropin-releasing hormone; EPA, Environmental Protection Agency; G-CSF, granulocyte colony-stimulating factor; GPx, glutathione peroxidase; GR, glutathione reductase; HOMA, homeostatic model assessment equation; HPA, hypothalamus–pituitary axis; IFN-γ, interferon-γ; IL, interleukin; IR, insulin resistance; MCP-1, monocyte chemoattractant protein-1; MDA, malondialdehyde; NAFLD, non-alcoholic fatty liver disease; NRF1, nuclear respiratory factor 1; POMC, proopiomelanocortin; ROS, reactive oxygen species; SHS, second-hand smoke; SOD, superoxide dismutase; TBA, thiobarbituric acid; TBARS, thiobarbituric acid reactive substances; THS, third-hand smoke; TNF-α, tumor necrosis factor α; TPM, total particulate matter; UCR-IACUC, University of California, Riverside, Institutional Animal Care and Use Committee.

References
1 Royal College of Physicians (2010) *Passive smoking and children. A report of the Tobacco Advisory Group of the Royal College of Physicians*, Royal College of Physicians, London
2 Willi, C., Bodenmann, P., Ghali, W., Faris, P. and Cornuz, J. (2007) Active smoking and the risk of type 2 diabetes in infants and children: a systematic review and meta-analysis. *JAMA* **298**, 2654–2664
3 Sleiman, M., Gundel, L.A., Pankow, J.F., Jacob, III, P., Singer, B.C. and Destaillats, H. (2010) Formation of carcinogens indoors by surface-mediated reactions of nicotine with nitrous acid, leading to potential thirdhand smoke hazards. *Proc. Natl. Acad. Sci. U.S.A.* **107**, 6576–6581
4 Matt, G., Quintana, P., Hovell, M., Bernert, T., Song, S., Noviant, N. et al. (2004) Households contaminated by environmental tobacco smoke: sources of infant exposures. *Tob. Control* **13**, 29–37
5 Protano, C., Andreoli, R., Manini, P. and Vitali, M. (2012) How home-smoking habits affect children: a cross-sectional study using urinary cotinine measurement in Italy. *Int. J. Public Health* **57**, 885–892
6 Martins-Green, M., Adhami, N., Frankos, M., Valdez, M., Goodwin, B., Lyubovitsky, J. et al. (2014) Cigarette smoke toxins deposited on surfaces: implications for human health. *PLoS ONE* **9**, e86391
7 Adhami, N., Starck, S.R., Flores, C. and Martins Green, M. (2016) A health threat to bystanders living in the homes of smokers: how smoke toxins deposited on surfaces can cause insulin resistance. *PLoS ONE* **11**, e0149510
8 Karim, Z.A., Alshbool, F.Z., Vemana, H.P., Adhami, N., Dhall, S., Espinosa, E.V. et al. (2015) Third-hand smoke: impact on hemostasis and thrombogenesis. *J. Cardiovasc. Pharmacol.* **66**, 177–182

Clinical Science (2017) **131** 2409–2426
DOI: 10.1042/CS20171053

9 Flores, C., Adhami, N. and Martins-Green, M. (2016) THS toxins induce hepatic steatosis by altering oxidative stress and SIRT1 levels. *J. Clin. Toxicol.* **6**, 318
10 Marrero, J.A., Fontana, R.J., Su, G.L., Conjeevaram, H.S., Emick, D.M. and Lok, A.S. (2002) NAFLD may be a common underlying liver disease in patients with hepatocellular carcinoma in the United States. *Hepatology* **36**, 1349–1354
11 Cazanave, S.C. and Sanyal, A.J. (2016) Molecular Mechanisms of Lipotoxicity in Nonalcoholic Fatty Liver Disease. *Hepatic De Novo Lipogenesis and Regulation of Metabolism*, Springer International Publishing
12 Tiniakos, D.G., Vos, M.B. and Brunt, E.M. (2010) Nonalcoholic fatty liver disease: pathology and pathogenesis. *Annu. Rev. Pathol.* **5**, 145–171
13 Roberts, J.W. and Dickey, P. (1995) Exposure of children to pollutants in house dust and indoor air. *Rev. Environ. Contam. Toxicol.* **143**, 59–78
14 Rehan, V.K., Sakurai, R. and Torday, J.S. (2011) Thirdhand smoke: a new dimension to the effects of cigarette smoke on the developing lung. *Am. J. Physiol. Lung Cell Mol. Physiol.* **301**, L1–L8
15 Dhall, S., Alamat, R., Castro, A., Sarker, A.H., Mao, J.H., Chan, A. et al. (2016) Tobacco toxins deposited on surfaces (third hand smoke) impair wound healing. *Clin. Sci. (Lond.)* **130**, 1269–1284
16 Teague Enterprises, http://www.teague-ent.com/equipment/smoking-machines
17 Huang, M.F., Lin, W.L. and Ma, Y.C. (2005) A study of reactive oxygen species in mainstream of cigarette. *Indoor Air* **15**, 135–140
18 Radi, R. (2004) Nitric oxide, oxidants, and protein tyrosine nitration. *Proc. Natl. Acad. Sci. U.S.A.* **101**, 4003–4008
19 Valenca, S.S., Silva Bezerra, F., Lopes, A.A., Romana-Souza, B., Marinho Cavalcante, M.C. et al. (2008) Oxidative stress in mouse plasma and lungs induced by cigarette smoke and lipopolysaccharide. *Environ. Res.* **108**, 199–204
20 Bolzan, A.D., Bianchi, M.S. and Bianchi, N.O. (1997) Superoxide dismutase, catalase and glutathione peroxidase activities in human blood: influence of sex, age and cigarette smoking. *Clin. Biochem.* **30**, 449–454
21 Ohtushi, M., Katsuoka, F., Koayashi, A., Aburatani, H., Hayes, J.D. and Yamamoto, M. (2008) NRF1 and NRF2 play distinct roles in activation of antioxiant response element-dependent genes. *J. Biol. Chem.*, doi:10.1074/jbc.M804597200
22 Chrousos, G.P. (1992) Regulation and dysregulatïon of the hypothalamic-pïtuitary-adrenal axis. The corticotropin-releasing hormone perspective. *Endocrinol. Metab. Clin. North Am.* **21**, 833–858
23 Whitnall, M.H. (1993) Regulation of the hypothalamic corticotropin-releasing hormone neurosecretory system. *Prog. Neurobiol.* **40**, 573–629
24 Rivier, C. and Vale, W. (1983) Modulation of stress-induced ACTH release by corticotropin-releasing factor, catecholamines and vasopressin. *Nature* **305**, 325–327
25 Pritchard, L.E., Turnbull, A.V. and White, A. (2002) Proopiomelanocortin processing in the hypothalamus: impact on melanocortin signalling and obesity. *J. Endocrinol.* **172**, 411–421
26 West, J.D. and Marnett, L.J. (2006) Endogenous reactive intermediates as modulators of cell signaling and cell death. *Chem. Res. Toxicol.* **19**, 173–194
27 Jiang, Y., Chen, C., Li, Z., Guo, W., Gegner, J.A., Lin, S. et al. (1996) Characterization of the structure and function of a new mitogen-activated protein kinase (p38β). *J. Biol. Chem.* **271**, 17920–17926
28 Ballif, B.A. and Blenis, J. (2001) Molecular mechanisms mediating mammalian mitogen-activated protein kinase (MAPK) kinase (MEK)-MAPK cell survival signals. *Cell Growth Differ.* **12**, 397–408
29 Lumeng, C. and Saltiel, A. (2011) Inflammatory links between, diet, obesity and metabolic disease. *J. Clin. Invest.* **121**, 2111–2117
30 illioja, S., Mott, D., Howard, B., Bennett, P., Yki-Jarvinen, H., Freymond, D. et al. (1988) Impaired skeletal muscle glucose tolerance as a disorder of insulin action: longitudinal and cross-sectional studies in Pima Indians. *N. Engl. J. Med.* **318**, 1217–1225
31 D'Autréaux, B. and Toledano, M.B. (2007) ROS as signalling molecules: mechanisms that generate specificity in ROS homeostasis. *Nat. Rev. Mol. Cell Biol.* **8**, 813–824
32 Dröge, W. (2002) Free radicals in the physiological control of cell function. *Physiol. Rev.* **82**, 47–95
33 Cooke, M., Evans, M., Dizdaroglu, M. and Lunec, J. (2003) Oxidative DNA damage: mechanisms, mutation, and disease. *FASEB J.* **17**, 1195–1214
34 Memişoğullari, R. and Bakan, E. (2004) Levels of lipid peroxidation in the serum of patients with Type 2 diabetes mellitus. *J. Diabetes Complications* **18**, 193–197
35 Rizza, R., Mandarino, L.J. and Gerich, J.E. (1982) Cortisol-induced insulin resistance in man: impaired suppression of glucose production and stimulation of glucose utilization due to a postreceptor defect of insulin action. *J. Clin. Endocrinol. Metab.* **55**, 131–138
36 Ducluzeau, P., Perretti, N., Laville, M., Andreelli, F., Vega, N., Riou, J. et al. (2010) Regulation by insulin of gene expression in human skeletal muscle and adipose tissue. Evidence for specific defects in type 2 diabetes. *Diabetes* **50**, 1134–1142
37 Francisco-Cruz, A., Aguilar-Santelises, M., Ramos-Espinosa, O., Mata-Espinosa, D., Marquina-Castillo, B. et al. (2014) Granulocyte-macrophage colony-stimulating factor: not just another haematopoietic growth factor. *Med. Oncol.* **31**, 774
38 Woolf, C.J., Allchorne, A., Safieh-Garabedian, B. and Poole, S. (1997) Cytokines, nerve growth factor and inflammatory hyperalgesia: the contribution of tumour necrosis factor alpha. *Br. J. Pharmacol.* **121**, 417–424
39 Nelms, K., Keegan, A. D., Zamorano, J., Ryan, J. J. and Paul, W. E. (1999) The IL-4 receptor: signaling mechanisms and biologic functions. *Annu. Rev. Immunol.* **17**, 701–738